Small activation entropy bestows high-stability of nanoconfined D-mannitol

Lin Cao(曹琳), Li-Jian Song(宋丽建), Ya-Ru Cao(曹亚茹), Wei Xu(许巍), Jun-Tao Huo(霍军涛), Yun-Zhuo Lv(吕云卓), and Jun-Qiang Wang(王军强)

Citation: Chin. Phys. B, 2021, 30 (**7**): 076103. DOI: 10.1088/1674-1056/abf919
Journal homepage: http://cpb.iphy.ac.cn; http://iopscience.iop.org/cpb

What follows is a list of articles you may be interested in

Characterization, spectroscopic investigation of defects by positron annihilation, and possible application of synthesized PbO nanoparticles

Sk Irsad Ali, Anjan Das, Apoorva Agrawal, Shubharaj Mukherjee, Maudud Ahmed, P M G Nambissan, Samiran Mandal, and Atis Chandra Mandal

Chin. Phys. B, 2021, 30 (**2**): 026103. DOI: 10.1088/1674-1056/abd2a9

Delta-doped quantum wire tunnel junction for highly concentrated solar cells

Ali Bahrami, Mahyar Dehdast, Shahram Mohammadnejad, Habib Badri Ghavifekr

Chin. Phys. B, 2019, 28 (**4**): 046102. DOI: 10.1088/1674-1056/28/4/046102

Confinement-induced modulation of elastic properties of nano-confined fluids in slit pore

Zong-Li Sun(孙宗利), Yan-Shuang Kang(康艳霜), Yan-Mei Kang(康艳梅)

Chin. Phys. B, 2019, 28 (**3**): 036102. DOI: 10.1088/1674-1056/28/3/036102

Zn-Cu-codoped SnO_2 nanoparticles:Structural, optical, and ferromagnetic behaviors

Syed Zulfiqar, Zainab Iqbal, Jianguo Lü(吕建国)

Chin. Phys. B, 2017, 26 (**12**): 126104. DOI: 10.1088/1674-1056/26/12/126104

Two waveguide layers in lithium niobate crystal formed by swift heavy Kr ion irradiation

Liu Tao, Huang Qing, Zhao Jin-Hua, Kong Wei-Jin, Liu Peng, Zhang Lian, Zhou Yu-Fan, Yu Xiao-Fei, Wang Lei, Wang Xue-Lin

Chin. Phys. B, 2015, 24 (**5**): 056102. DOI: 10.1088/1674-1056/24/5/056102

Small activation entropy bestows high-stability of nanoconfined D-mannitol*

Lin Cao(曹琳)[1,2,3], Li-Jian Song(宋丽建)[2,3,†], Ya-Ru Cao(曹亚茹)[2,3], Wei Xu(许巍)[2,3], Jun-Tao Huo(霍军涛)[2,3], Yun-Zhuo Lv(吕云卓)[1,‡], and Jun-Qiang Wang(王军强)[2,3,§]

[1] School of Materials Science and Engineering, Dalian Jiaotong University, Dalian 116028, China
[2] CAS Key Laboratory of Magnetic Materials and Devices, and Zhejiang Province Key Laboratory of Magnetic Materials and Application Technology, Ningbo Institute of Materials Technology and Engineering, Chinese Academy of Sciences (CAS), Ningbo 315201, China
[3] Center of Materials Science and Optoelectronics Engineering, University of Chinese Academy of Sciences, Beijing 100049, China

(Received 8 March 2021; revised manuscript received 6 April 2021; accepted manuscript online 19 April 2021)

It has been a long-standing puzzling problem that some glasses exhibit higher glass transition temperatures (denoting high stability) but lower activation energy for relaxations (denoting low stability). In this paper, the relaxation kinetics of the nanoconfined D-mannitol (DM) glass was studied systematically using a high-precision and high-rate nanocalorimeter. The nanoconfined DM exhibits enhanced thermal stability compared to the free DM. For example, the critical cooling rate for glass formation decreases from 200 K/s to below 1 K/s; the T_g increases by about 20 K–50 K. The relaxation kinetics is analyzed based on the absolute reaction rate theory. It is found that, even though the activation energy E^* decreases, the activation entropy S^* decreases much more for the nanoconfined glass that yields a large activation free energy G^* and higher thermal stability. These results suggest that the activation entropy may provide new insights in understanding the abnormal kinetics of nanoconfined glassy systems.

Keywords: D-mannitol glass, confinement, relaxation, activation entropy

PACS: 61.43.Fs, 61.20.Lc, 64.70.P– **DOI:** 10.1088/1674-1056/abf919

1. Introduction

The nanoconfined glasses usually exhibit enhanced thermal properties compared to the free glasses, *e.g.*, higher glass transition temperature[1–4] and depressed crystallization kinetics.[5,6] For molecular glasses, the hydrogen bonds are depressed in nanoconfinement that can significantly improve the stability of small molecular glass,[7] which may be helpful in promoting the applications of amorphous drugs.[8] However, such changes in thermal properties depend on kinds of experimental factors, *e.g.*, nanoporous material, the size of the nanopores or the dimensionality. It is still heavily debated for the physical origins of the enhanced thermal properties of nanoconfined glasses.

The activation energy E^* of relaxations is usually used for evaluating the kinetic stability, which can be calculated by measuring the heating rate dependent behaviors.[9–14] But it is puzzling that a glass with the higher glass transition temperature, which denotes a higher kinetic stability, may have the same activation energy for α relaxation as the glass with a much lower glass transition temperature, which denotes a lower kinetic stability.[15] This suggests that the activation energy may not be the sole parameter for evaluating the relaxation kinetics. For the absolute reaction rate theory, one reaction process should contain the potential energy position and the configuration of this path, which correspond to the activation enthalpy H^* and the activation entropy S^*, respectively. The activation energy E^* shares a linear relationship with the H^*.[16] The S^* reflects the distortion degree of the transition state and can be a positive value or even negative value.[17,18] Therefore, considering both the relaxation enthalpy and relaxation entropy is helpful to understand the physical origin of the abnormal relaxation kinetics of confined glasses.

D-mannitol (DM) is a kind of natural hexahydric alditol and has been widely used in pharmaceutical, excipient, and sugar substitute.[19] The amorphous pharmaceuticals are of special interests because of their faster dissolving rate and higher solubility compared to the crystalline counterparts.[20,21] However, the hydrogen bonds can cause the crystallization.[22] Even though the usual glassy DM can transform into a glassy phase X via a polyamorphism transition that has a higher glass transition temperature, the crystallization behavior of the glassy phase X remains unchanged.[23] Thus, it is intriguing to study the possibility of achieving a higher stable glassy state of DM by nanoconfinement, and it is interesting to reveal the physical origins for the possible

*Project supported by the National Natural Science Foundation of China (Grant Nos. 52001319, 52071327, 51922102, 51771216, and 51701230), the Natural Science Foundation of Zhejiang Province, China (Grant Nos. LR18E010002), the Ningbo 2025 Science and Technology Innovation Project (Grant No. 2019B10051), and the Natural Science Foundation of Ningbo City (Grant No. 202003N4354).

†Corresponding author. E-mail: songlj@nimte.ac.cn
‡Corresponding author. E-mail: yunzhuohit@gmail.com
§Corresponding author. E-mail: jqwang@nimte.ac.cn

changes in thermal properties.

In this work, the kinetics of the nanoconfined DM glass is studied by using a high-precision high-rate differential scanning calorimeter. The activation energy E^* and the activation enthalpy H^* decreased, while the activation free energy G^* increases for the nanoconfined DM that is attributed to the large decreases in S^*. Meanwhile, the small S^* suggests that the strong attraction of DM may occur at the Au layer and cause the higher glass transition temperature. And the S^* sheds a new light on understanding the thermal stability of nanoconfined glasses.

2. Experimental details

D-mannitol (purity $>$ 99 wt.%) was purchased from Sigma Company. The master alloy ingot $Ag_{100-x}Au_x$ ($x = 10$, 20, 35) was prepared by arc melting under a high-purity argon atmosphere. Then the as-spun ribbons were prepared by a copper roller melt-spinning method with a tangent speed of 40 m/s. After that, the ribbons were kept in 70% concentrated nitric acid at 323 K for 3600 s to dealloyed the Ag in the ribbons to obtain nanoporous Au. The nanoporous Au was put on a hot stage at $T = 440$ K. The DM was put on the surface of nanoporous Au little by little. As the good wetting between DM melt and Au, the DM melt will penetrate into the nanopores. When the nanopores are not filled completely, the surface looks 'dry'; when the nanopores are filled completely, the surface looks a bit 'wet'. Then, the sample is laid on the hot stage for a while to let the extra DM on the surface to evaporate till it becomes dry again. A high-rate differential scanning calorimeter (Mettler Toledo Flash DSC 1) was used to study the thermal properties of the free and confined DM. Before measurement, the sample was first heated to 446 K (6 K above the melting temperature) and hold for 5 s to allow the sample to have good contact with the chip. To obtain the relaxation kinetics of free and confined DM, the sample was annealed at $T_a = 273$ K for various time $t_a = 0.1$ s–10000 s. The relaxation peak was measured at the heating rate $R_h = 100$, 200, 500, and 1000 K/s. The high-purity argon gas (40 mL/min) was introduced to prevent oxidation of the sample. The morphologies of nanopores Au and the confined DM were examined using a scanning electronic microscope (SEM, Thermo scientific, Verios G4 UC). The molecular vibration spectrum was investigated using Fourier Transform Infrared Spectrometer (FTIR, Thermo Nicolet 6700).

3. Results and discussion

The structure of $Au_{10}Ag_{90}$, $Au_{20}Ag_{80}$, and $Au_{35}Ag_{65}$ after dealloying was recorded using SEM [Figs. 1(a)–1(c)]. The nanoporous structure distributed homogeneously. The typical size of the nanopores has been marked by the arrows in Figs. 1(a)–1(c), which is determined as about (44 ± 11) nm (Au_{10}), (35 ± 8) nm (Au_{20}), and (22 ± 3) nm (Au_{35}), respectively. The SEM images in Figs. 1(d)–1(f) confirm that the nanoconfined DM has a homogeneous structure that the nanopores have been filled by the DM uniformly.

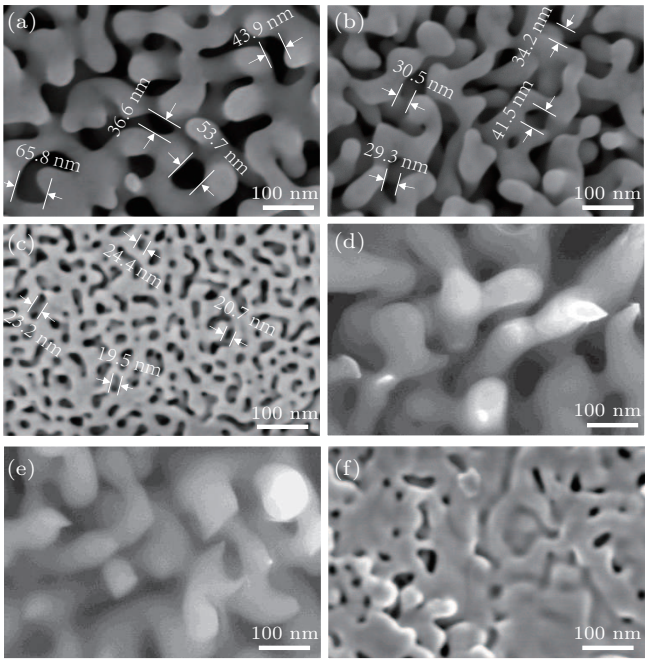

Fig. 1. Scanning electron microscope (SEM) images of (a)–(c) empty nanoporous Au prepared by dealloying Au_xAg_{100-x} ($x = 10$, 20, 35), the size of the nanopores is determined to be about (44 ± 11) nm (Au_{10}), (35 ± 8) nm (Au_{20}), and (22 ± 3) nm (Au_{35}), respectively; (d)–(f) D-mannitol confined in nanoporous Au.

The representative heat flow traces for free and confined DM upon cooling at various cooling rates were measured [Figs. 2(a)–2(d)]. For free DM, the liquid solidifies into crystals at a temperature T_s when the cooling rate $R_c \leq 200$ K/s while the glass was formed when $R_c > 200$ K/s. However, the solidification of melt was suppressed greatly during nanoconfinement. To compare the effect of nanoconfinement on the solidification, the critical cooling rate was measured by the reduced enthalpy H_s [Fig. 2(e)]. The critical cooling rate is determined to be about 200 K/s, 10 K/s, 2 K/s, and less than 1 K/s for the free, Au_{10}, Au_{20}, and Au_{35} DM, respectively. That is to say, the confinement can significantly enhance the glass-forming ability for DM.

The phase transition kinetics of free and confined DM upon heating are studied at various heating rates further [Figs. 3(a)–3(d)]. For all heating rates, the free DM experiences the glass, crystallization and melting. In contrast, the crystallization and melting can be detected for the confined DM (Au_{10}) at low heating rate $R_h \leq 100$ K/s, while the Au_{20} and Au_{35} undergo the glass to liquid transition without crystallization and melting of crystals. The glass transition temperature (T_g) of free and confined DM shifts to high temperature with the increase of the heating rates. At a given heating rate $R_h = 1000$ K/s, the T_g is about 295 K for free DM and the T_g

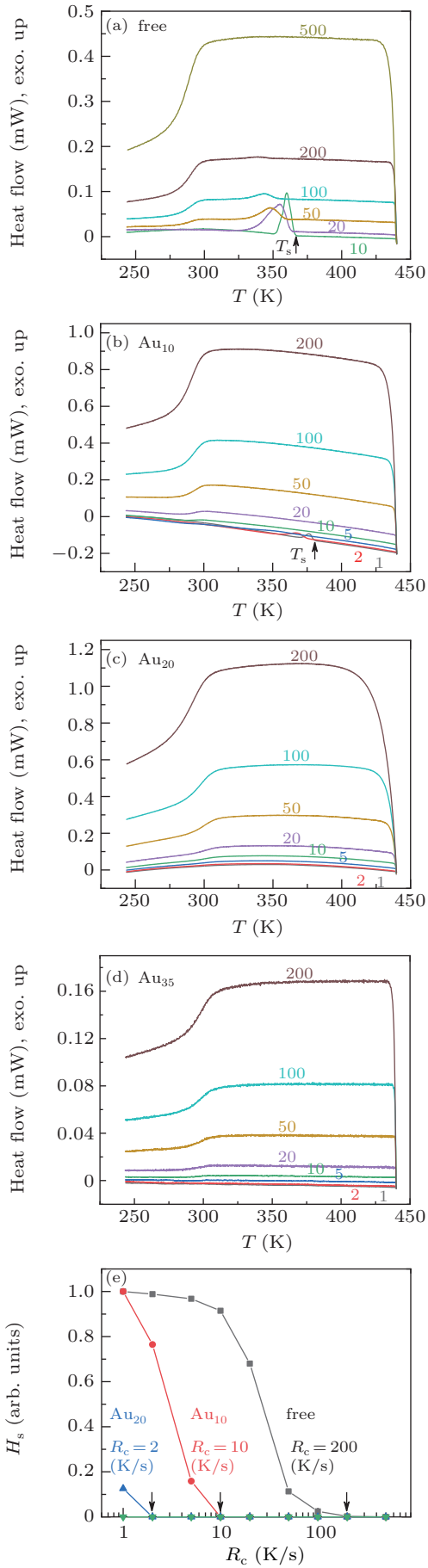

Fig. 2. The DSC traces of (a) free D-mannitol and (b)–(d) confined D-mannitol at various cooling rates. (e) The enthalpy of solidification *versus* cooling rate. The critical cooling rates are marked by the arrows.

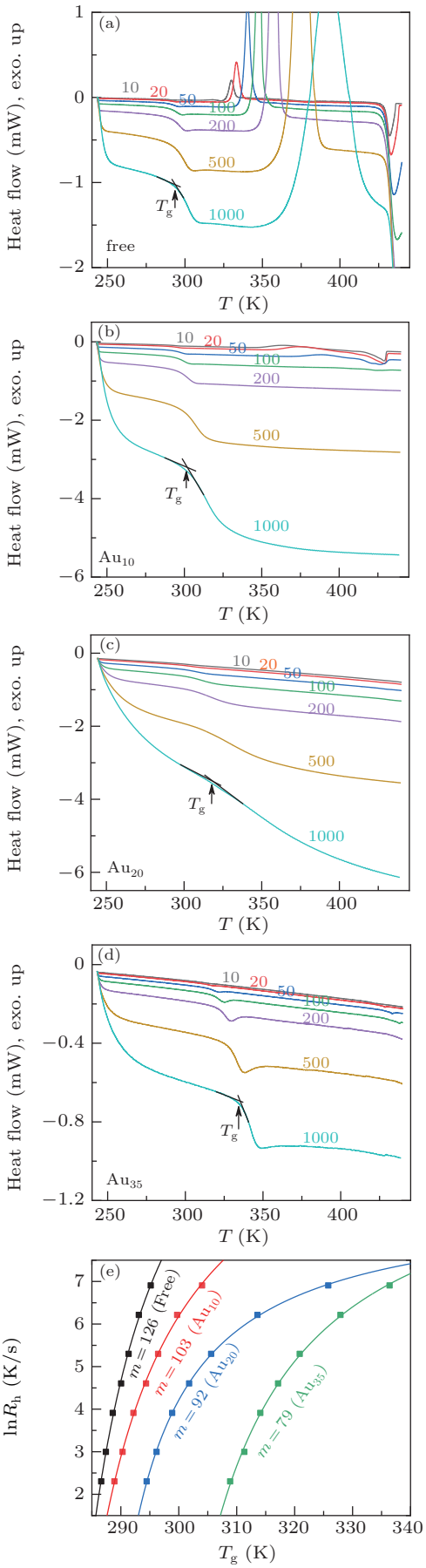

Fig. 3. The DSC traces of (a) free D-mannitol and (b)–(d) confined D-mannitol at various heating rates and subsequently cooled at 1000 K/s. (e) The heating rate *versus* glass transition temperature, the solid lines are the fitting results by VFT equation.

increases from 295 K to 336 K when the nanopore size decreases from 44 nm to 22 nm. In Fig. 3(e), the glass transition temperature changes with heating rate in thermal signal follows the Vogel–Fulcher–Tammann (VFT) equation[24,25]

$$\ln R_{\rm h} = \ln A + \frac{DT_0}{(T - T_0)}, \tag{1}$$

where $R_{\rm h}$ is the heating rate, A is the pre-factor, D is the strength parameter, T_0 is the asymptotic value of $T_{\rm g}$ at infinitely slow cooling/heating rate.[20,21] The $T_{\rm g}$ at heating rate $R_{\rm h} = 10$ K/min is estimated by extrapolating the VFT equation. From the VFT fitting parameter, the fragility was calculated by[26]

$$m = \frac{DT_0T_{\rm g}}{(T_{\rm g} - T_0)^2 \ln 10}. \tag{2}$$

The fragility m is about 103 ± 1, 92 ± 1, and 79 ± 1 for nano pore size 44 nm, 35 nm, and 22 nm, respectively. This result proves the abnormal reduction of kinetics barrier.

Figures 2 and 3 show that, when the D-mannitol glass is confined in nanopores, both the thermal stability of undercooled liquid against crystallization (equal to glass forming ability) and the thermal stability of glassy solid against glass transition increase. This suggests a positive relationship between the two stabilities. Generally speaking, a high glass forming ability is usually related to a small melting entropy $\Delta S_{\rm m}$[27,28] and a larger $T_{\rm g}/T_{\rm L}$ ($T_{\rm g}$ is the glass transition temperature, $T_{\rm L}$ is the liquidus temperature).[29] That is, $\Delta S_{\rm m} \propto T_{\rm L}/T_{\rm g}$. Thus, for a given $T_{\rm L}$, a high thermal stability of undercooled liquid against crystallization (small $\Delta S_{\rm m}$ and good glass forming ability) is related to the high thermal stability of glassy solid against glass transition (high $T_{\rm g}$).

To study the reduced kinetics behavior carefully, the thermal stability of free and confined DM at annealing temperature $T_{\rm a} = 273$ K for various time is revealed. In Fig. 4(a), the heat flow curves of annealed Au_{35} sample were measured at heating rate $R_{\rm h}$ =200 K/s and the annealing times $t_{\rm a} = 0.1$ s–10000 s. The relaxation peak gradually shifts to the high temperature and the amplitude becomes larger with the increase of the annealing time. By subtracting the heat flow curve of the quenched sample from the heat flow curves of annealed sample, the relaxation peak curves at different heating rates ($R_{\rm h} = 100$, 200, 500, and 1000 K/s) for $t_{\rm a} = 5000$ s are obtained [Fig. 4(b)]. The heating rate *versus* the relaxation peak temperature is studied by the Kissinger plot,[30]

$$\ln \frac{R_{\rm h}}{T^2} = C - \frac{E^*}{RT}, \tag{3}$$

where C is the constant. In Fig. 4(c), the $\ln(R_{\rm h}/T^2)$ is plotted *versus* $1/T_{\rm p}$ for the relaxed samples. The activation energy (E^*) of the corresponding relaxation state is calculated by fitting the slope of the data [Fig. 4(d)]. For free DM, the activation energy is about 71 kJ/mol in the initial annealing stage, which is approximately equal to the activation energy

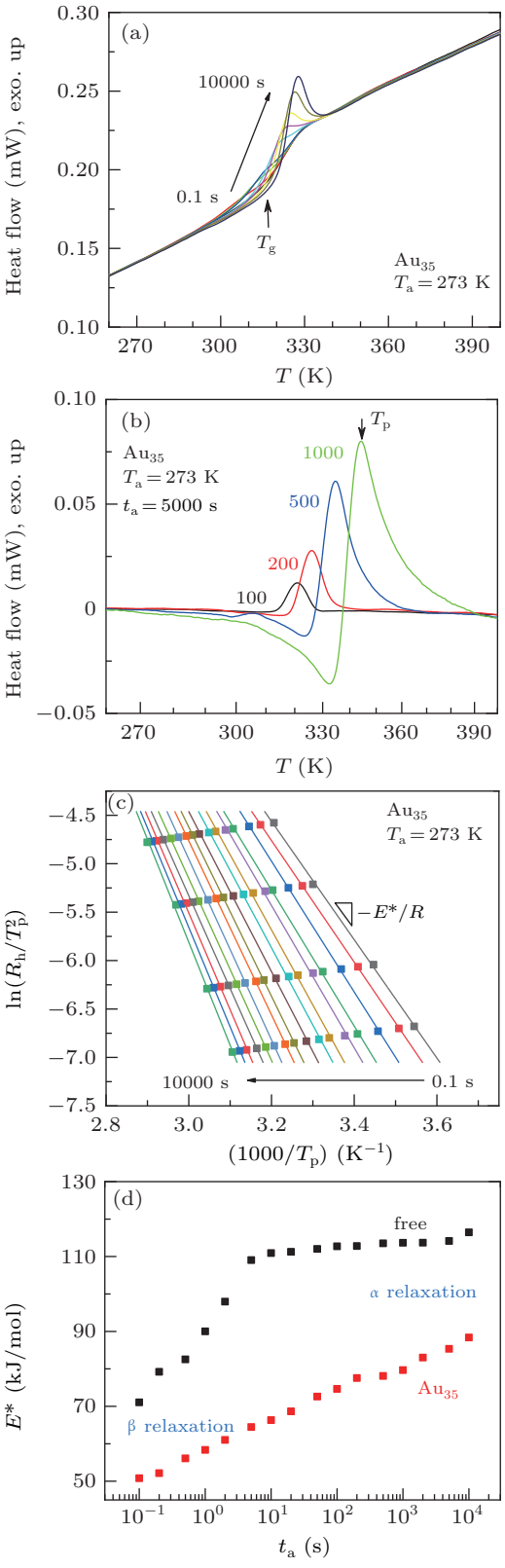

Fig. 4. (a) The DSC curve of restricted D-mannitol annealed at $T_{\rm a} = 273$ K for different annealing time ($t_{\rm a} = 0.1$ s–10000 s), the heating rate is 200 K/s. (b) The relaxation peaks of the confined D-mannitol measured at different heating rates ($R_{\rm h} = 100$, 200, 500 and 1000 K/s), $T_{\rm a} = 273$ K and $t_{\rm a} = 5000$ s. (c) Kissinger plot of the relaxation peak temperatures $T_{\rm p}$ for sample annealed at 273 K, and the annealing time $t_{\rm a} = 0.1$ s–10000 s. The relaxation activation energy E^* is determined by the slope. (d) The activation energy E^* *versus* annealing time for free D-mannitol and confined D-mannitol at 273 K.

of β relaxation $E^*_\beta \approx 26RT_g \approx 61$ kJ/mol (given $T_g = 284$ K at 10 K/min).[23] Along with the increase of annealing time, the activation energy gradually increases to about 116 kJ/mol, which is close to the E^* of α relaxation.[7] Such a two-step relaxation phenomenon during isothermal annealing have been observed in polymer, basalt glass and metallic glasses.[31–35] For the Au_{35} nanoconfined glass, the relaxation barrier is much smaller than the free glass and exhibits similar transition. The activation energy of β relaxation is about 50 kJ/mol, which is 28% lower than that of free DM, and the activation energy of α relaxation is about 88 kJ/mol, which is 24% lower than that of free DM [Fig. 4(d)].

The absolute reaction rates theory consider the configuration of atoms at the transition state. It is given as[36,37]

$$\ln\frac{R_h}{T_p^3} = -\frac{H^*}{RT_p} + \ln\frac{kR}{h_P} + \ln\frac{1}{H^*} + \frac{S^*}{R}, \tag{4}$$

where k is the Boltzmann constant, R is the gas constant, h_P is the Planck constant, H^* is the activation enthalpy, and S^* is the activation entropy. Figure 5(a) shows the change of T_p with the heating rate. In Fig. 5(b), the H^* also exhibits two-step transition behavior, and satisfies $E^* = H^* + RT_p$, where T_p is measured at $R_h = 100$ K/s.[37,38] The S^* decreases greatly when the sample was confined [Fig. 5(c)]. The H^* decreases by about 0.3 times, while S^* decreases by more than 10 times, even transforms from positive to negative. The small S^* reflects the relaxation paths were blocked and the confined sample tends to the liquid state. Although the H^* of free sample is higher than that of confined sample, activation free energy $G^* = H^* - T_pS^*$ exhibits an opposite trend, indicating that the G^* can reflect the kinetics stability more carefully than the E^* and H^* [Fig. 5(d)].

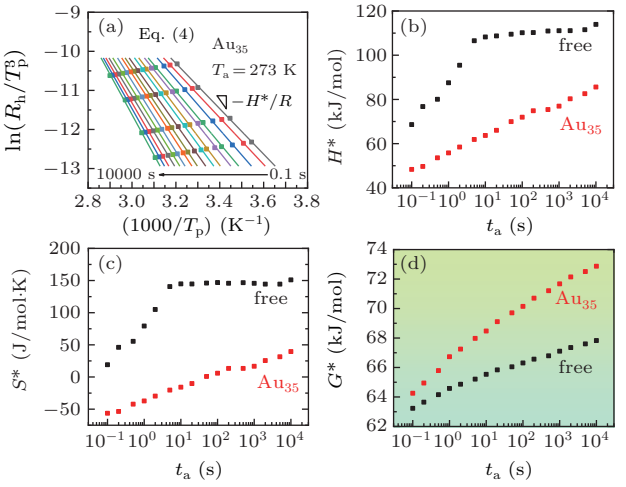

Fig. 5. (a) The absolute reaction rate theory analyses of the relaxation peak temperatures T_p for sample annealed at 273 K for various time $t_a = 0.1$ s–10000 s. (b) Activation enthalpy H^* *versus* annealing time for samples annealed at T_a =273 K. (c) Activation enthalpy S^* as a function of annealing time. (d) Activation free energy G^* *versus* annealing time t_a for free D-mannitol and confined D-mannitol at $T_a = 273$ K.

In order to explore the effect of confinement on the interaction between molecules, FTIR experiments were performed. The vibration spectra of O–H and C–H stretching models in the fundamental frequency region (2500 cm^{-1}–4000 cm^{-1}) are shown in Fig. 6. The O–H stretching peak of crystalline DM is narrower than the glassy DM, but broader than the confined samples. And the narrower O–H stretching models of the confined samples should be caused by the suppression of hydrogen bonds.[7] The enhanced glass forming ability may be attributed to the suppression of hydrogen bonds, which is consistent with other works.[39–41] After confinement, the S^* becomes negative, which suggests a relaxation-induced disordering phenomenon. The negative activation entropy is beneficial to retain the liquid state and high resistance to crystallization. We can speculate that the suppression of hydrogen bonds under the confinement reduce the relaxation paths (small S^*), which enhance the kinetics stability and improve the resistance to crystallization.

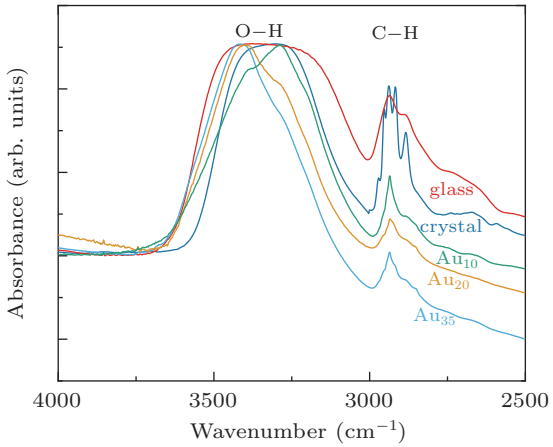

Fig. 6. The infrared spectra of O–H and C–H stretching modes for free glassy D-mannitol (glass), crystalline D-mannitol (crystal), and nanoconfined D-mannitol (Au_{10}, Au_{20}, and Au_{35}).

The finding of confinement effect provides a chance to understand the novel and complex kinetics in glass and crystal for nanoscience.[42–47] Previous results point out that the nanometer length scale promotes the faster dynamics, which will decrease the glass transition temperature.[48–50] Besides, the strong attractive interaction between material and nanoporous will impede the motion of atoms and enhance the glass transition temperature.[51] The small activation entropy for nanoconfined glass denotes that the large cooperative motions during relaxation is depressed, which induces the higher glass transition temperature. In the annealing experiment, phase X is not observed, which is contrary to the free DM glass.[52] The frustration of the nucleation of phase X could also be attributed to the depressed cooperative molecular motions.

4. Conclusion and perspectives

In this work, we studied the effect of nanoconfinement on glassy D-mannitol carefully. The critical cooling rate for glass formation decreases from 200 K/s for free DM to below 1 K/s,

the T_g increases by about 20 K–50 K for the nanoconfined DM. However, the fragility, isothermal relaxation activation energy decreases by about 20%–40% after confinement. The underlying physical mechanism is studied based on the absolution reaction rate theory. Unlike the decrease in activation energy, the activation free energy increases for the nanoconfined glass owing to the large decrease in activation entropy. These results shed new lights on understanding the relaxation and crystallization processes for nanoconfined glasses.

References

[1] Zhao H Y, Yu Z N, Begum F, Hedden R C and Simon S L 2014 *Polymer* **55** 4959
[2] Wang H N, Hor J L, Zhang Y, Liu T Y, Lee D and Fakhraai Z 2018 *ACS Nano* **12** 5580
[3] Casalini R, Zhu L, Baer E and Roland C M 2016 *Polymer* **88** 133
[4] Schüller J, Mel'nichenko Y B, Richert R and Fischer E W 1994 *Phys. Rev. Lett.* **73** 2224
[5] Cheng S X and McKenna G B 2019 *Mol. Pharm.* **16** 856
[6] Dai X Y, Li H H, Ren Z J, Russell T P, Yan S K and Sun X L 2018 *Macromolecules* **51** 5732
[7] Cao Y R, Song L J, Li A, Huo J T, Li F S, Xu W and Wang J Q 2020 *Sci. China-Phys. Mech. Astron.* **63** 276113
[8] Laitinen R, Löbmann K, Strachan C J, Grohganz H and Rades T 2013 *International Journal of Pharmaceutics* **453** 65
[9] Angell C A 1985 *J. Non-Cryst. Solids* **73** 1
[10] Angell C A 1995 *Science* **267** 1924
[11] Jo C L, Xia L, Ding D and Dong Y D 2006 *Chin. Phys. Lett.* **23** 672
[12] Zhao L Z, Xue R J, Wang W H and Bai H Y 2017 *Chin. Phys. B* **26** 018106
[13] Zhang F F, Chen Y M, Wang R P, Shen X, Wang J Q and Xu T F 2019 *Chin. Phys. B* **28** 047802
[14] Wang J F, Liu L, Pu J and Xiao J Z 2004 *Acta Phys. Sin.* **53** 1916 (in Chinese)
[15] Qin Q and McKenna G B 2006 *J. Non-Cryst. Solids* **352** 2977
[16] Michaelides A, Liu Z P, Zhang C J, Alavi A, King D A and Hu P 2003 *J. Am. Chem. Soc.* **125** 3704
[17] Zarra S, Smulders M M J, Lefebvre Q, Clegg J K and Nitschke J R 2012 *Angew. Chem. Int. Ed.* **51** 6882
[18] Rozwadowski T, Jasiurkowska-Delaporte M, Massalska-Arodź M, Yamamura Y and Saito K 2020 *Phys. Chem. Chem. Phys.* **22** 24236
[19] Su W Y, Jia N, Li H S, Hao H X and Li C L 2017 *Chin. J. Chem. Eng.* **25** 358
[20] Zhang P, Forsgren J and Strømme M 2014 *Int. J. Pharmaceut.* **472** 185
[21] Yu L 2001 *Adv. Drug. Deliver. Rev.* **48** 27
[22] Wibowo E S, Park B D and Causin V 2020 *Ind. Eng. Chem. Res.* **59** 13095
[23] Zhu M, Wang J Q, Perepezko J H and Yu L 2015 *J. Chem. Phys.* **142** 244504
[24] Brüning R and Samwer K 1992 *Phys. Rev. B* **46** 11318
[25] Zhang B, Wang R J, Zhao D Q, Pan M X and Wang W H 2004 *Phys. Rev. B* **70** 224208
[26] Böhmer R, Ngai K L, Angell C A and Plazek D J 1993 *J. Chem. Phys.* **99** 4201
[27] Wang L M, Liu R P and Tian Y J 2020 *Acta Phys. Sin.* **69** 196401 (in Chinese)
[28] Wang L M, Tian Y J, Liu R P and Wang W H 2012 *Appl. Phys. Lett.* **100** 261913
[29] Turnbull D 1969 *Contemp. Phys.* **10** 473
[30] Chen H S 1981 *J. Non-Cryst. Solids* **46** 289
[31] Gallino I, Cangialosi D, Evenson Z, Schmitt L, Hechler S, Stolpe M and Ruta B 2018 *Acta Mater.* **144** 400
[32] Hornbøll L and Yue Y Z 2008 *J. Non-Cryst. Solids* **354** 350
[33] Perez-De-Eulate N G and Cangialosi D 2018 *Macromolecules* **51** 3299
[34] Cangialosi D, Boucher V M, Alegria A and Colmenero J 2013 *Phys. Rev. Lett.* **111** 095701
[35] Song L J, Xu W, Huo J T, Wang J Q, Wang X M and Li R W 2018 *Intermetallics* **93** 101
[36] Cagle Jr F W and Eyring H 1951 *J. Appl. Phys.* **22** 771
[37] Song L J, Xu W, Huo J T, Li F S, Wang L M, Ediger M D and Wang J Q 2020 *Phys. Rev. Lett.* **125** 135501
[38] Starkweather H W 1981 *Macromolecules* **14** 1277
[39] Kuo S W, Chan S C and Chang F C 2003 *Macromolecules* **36** 6653
[40] Ma Y N, Zhou T, Su G H, Li Y and Zhang A M 2016 *RSC Adv.* **6** 87405
[41] Yu H B and Yang Q 2017 *Acta Phys. Sin.* **66** 176108 (in Chinese)
[42] Ha J M, Wolf J H, Hillmyer M A and Ward M D 2004 *J. Am. Chem. Soc.* **126** 3382
[43] Ha J M, Hillmyer M A and Ward M D 2005 *J. Phys. Chem. B* **109** 1392
[44] Beiner M, Rengarajan G T, Pankaj S, Enke D and Steinhart M 2007 *Nano Lett.* **7** 1381
[45] Rengarajan G T, Enke D, Steinhart M and Beiner M 2011 *Phys. Chem. Chem. Phys.* **13** 21367
[46] Jackson C L and McKenna G B 1991 *J. Non-Cryst. Solids* **131** 221
[47] Sonnenberger N, Anders N, Golitsyn Y, Steinhart M, Enke D, Saalwächter K and Beiner M 2016 *Chem. Commun.* **52** 4466
[48] Arndt M, Stannarius R, Groothues H, Hempel E and Kremer F 1997 *Phys. Rev. Lett.* **79** 2077
[49] Schönhals A, Goering H, Schick C, Frick B and Zorn R 2003 *Eur. Phys. J. E* **12** 173
[50] Beiner M and Huth H 2003 *Nat. Mater.* **2** 595
[51] Zuo Y C, Zhang Y Z, Huang R D and Min Y J 2019 *Phys. Chem. Chem. Phys.* **21** 22
[52] Tang W and Perepezko J H 2018 *J. Chem. Phys.* **149** 074505